Satellite Navigation and Space Geodesy:
Recent Progresses and Perspective

Shuanggen Jin[1, 2], S.H. Kutogluh[1], C. Mekik[1]

[1] Department of Geomatics Engineering, Bulent Ecevit University, Zonguldak, Turkey

[2] Shanghai Astronomical Observatory, Chinese Academy of Sciences, Shanghai, China

Email: sgjin@shao.ac.cn; sgjin@beun.edu.tr

Website: http://www.shao.ac.cn/geodesy

Sofia, Bulgaria,
May 2015

Outline

- Introduction
- Geodetic Observations & Results
- Questions and Challenges

1. Introduction

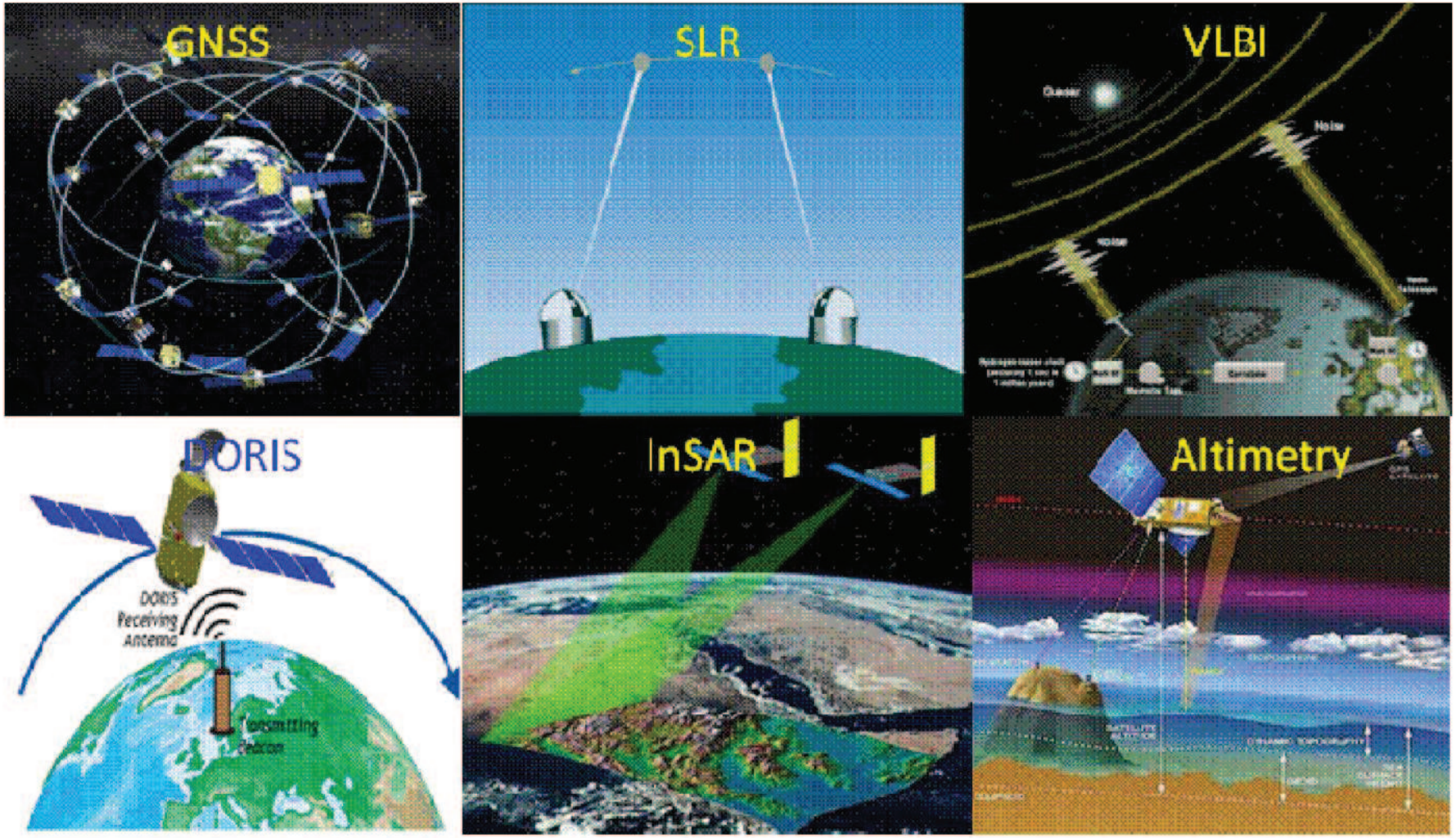

Fig. 1. Main space geodetic techniques.

Roles of each space geodetic technique

Table 1
Roles and uses of each space geodetic technique.

Parameters	GNSS	VLBI	DORIS	SLR	LLR	Altimetry	InSAR/LiDAR	Gravimetry
ICRF		√						
ITRF	√	√	√	√	√	(√)	(√)	(√)
Polar motion	√	√	√	√	√			(√)
Nutation	(√)	√		(√)	√			
UT1		√						
Length of day	√	√	√	√	√			(√)
Geocenter	√		√	√		(√)		√
Gravity field	√	√	√	√	(√)	√		√
Plate motion	√	√	√	√	(√)	(√)	√	√
LEO orbits	√	√	√	√	√	√		
Navigation/orbit	√	√	√	√	√	√		
Timing and clock	√	√		(√)				
Ionosphere	√	√	√			√	√	
Troposphere	√	√	√			√	√	
Hydrology	√					√	√	√
Oceans	√					√	√	√

Space geodesy and Earth System Interaction

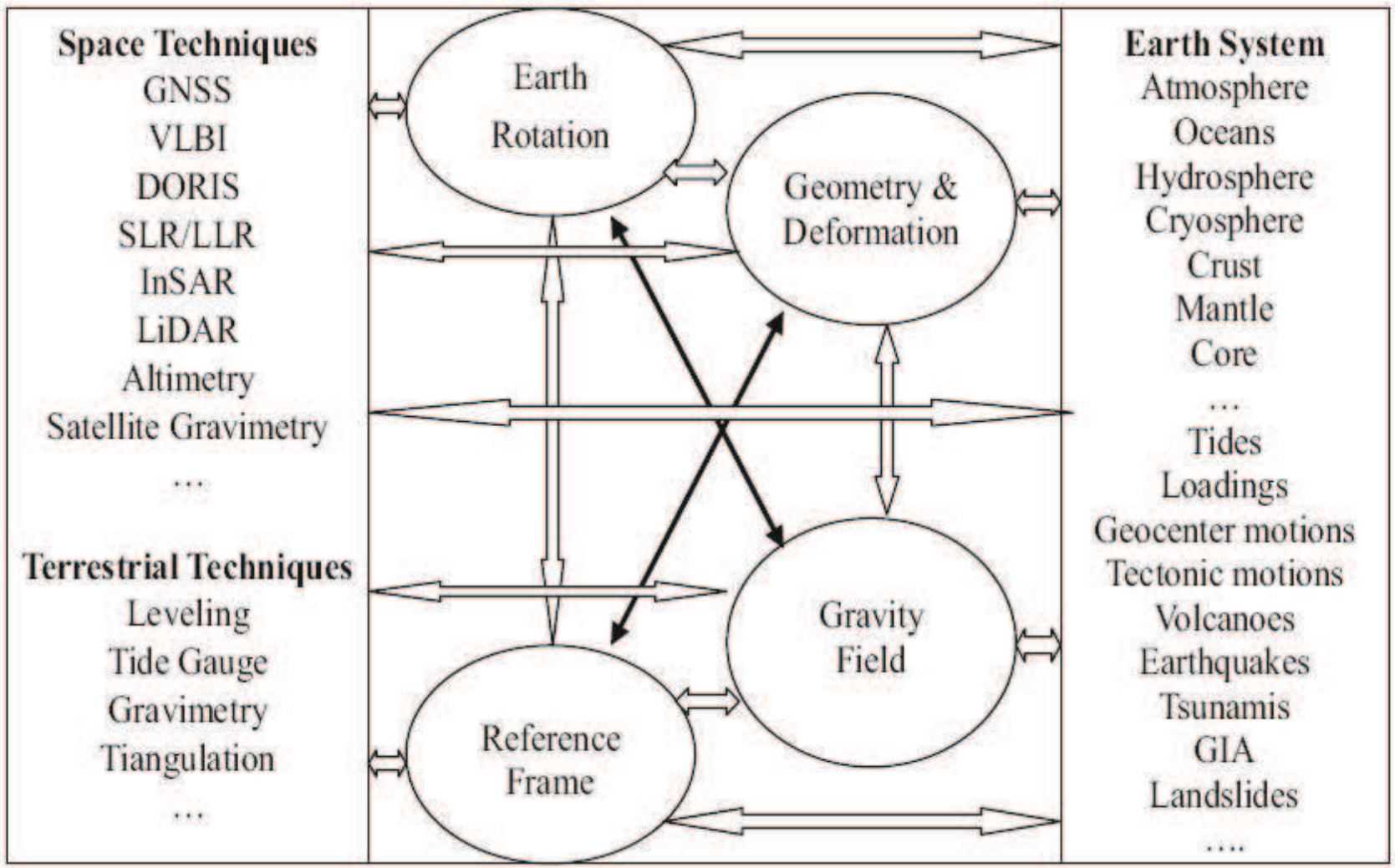

2. Geodetic Observations and Results

2.1) Atmospheric Sounding

2.2) Ocean Remote Sensing

2.3) Hydrological Remote Sensing

2.4) Crustal Deformation Monitoring

2.1 Atmospheric Sounding

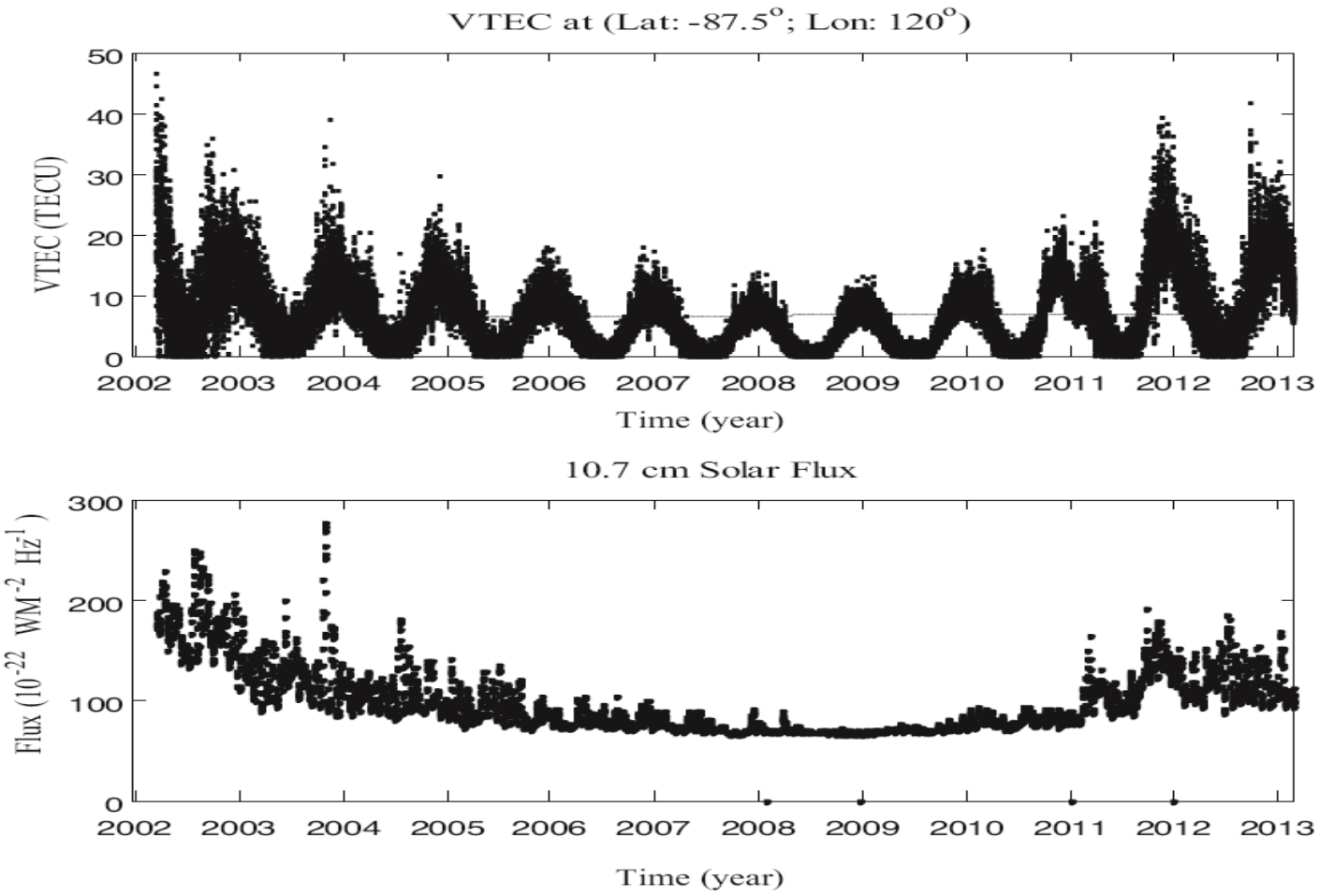

Fig. 4. Vertical TEC (VTEC) time series at (120 E°, −87.5 S°) and 10.7 cm Solar Flux.

Jin et al., J. Geodyn., 2013

GNSS Meteorology/Climatology

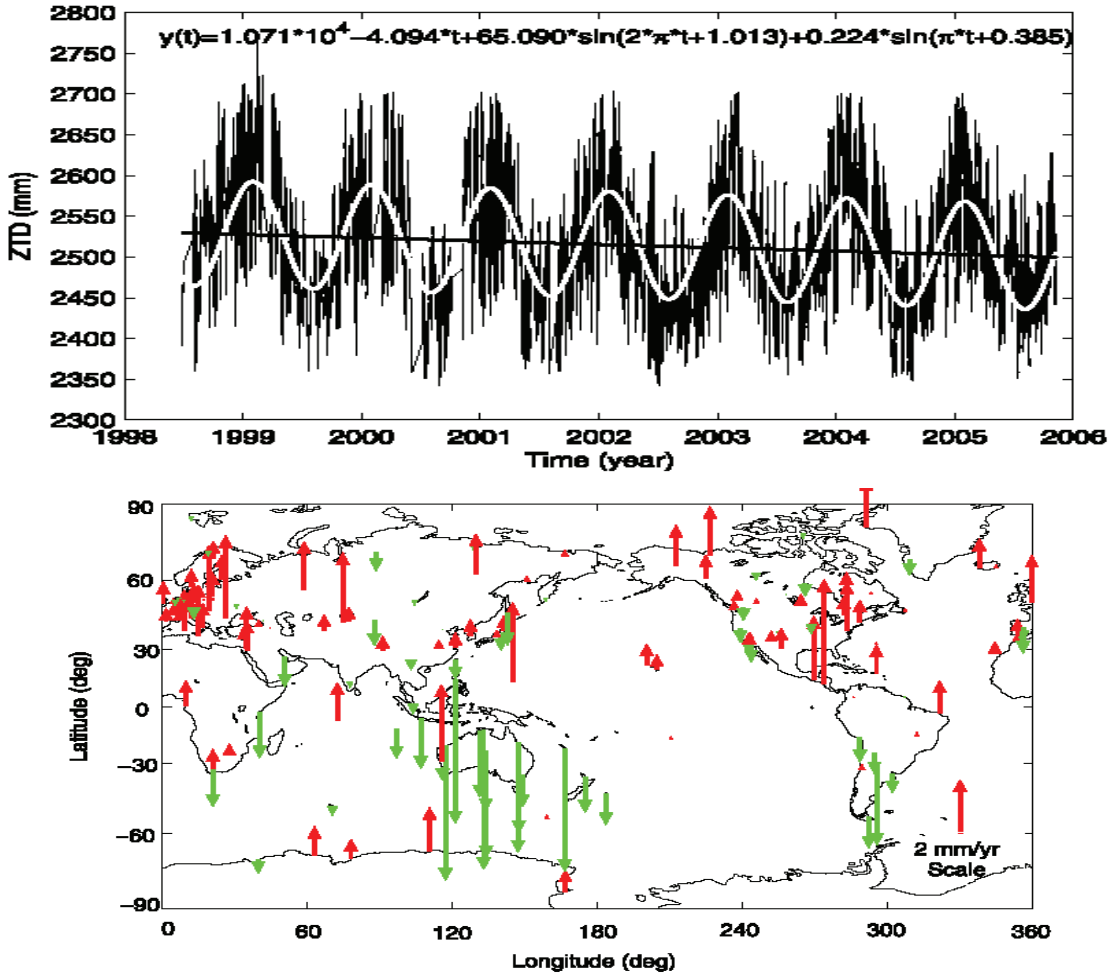

Figure 9. Secular variation trend of ZTD at global IGS sites. The red upward arrows represent the increase of secular ZTD variations, and the green downward arrows stand for the decrease of secular ZTD variations.

Jin et al., J.Geophys. Res., 2007

e.g., 3-D ionopsheric behaviours during the larger geomagnetic storms—A case of November 20 2003 storm.

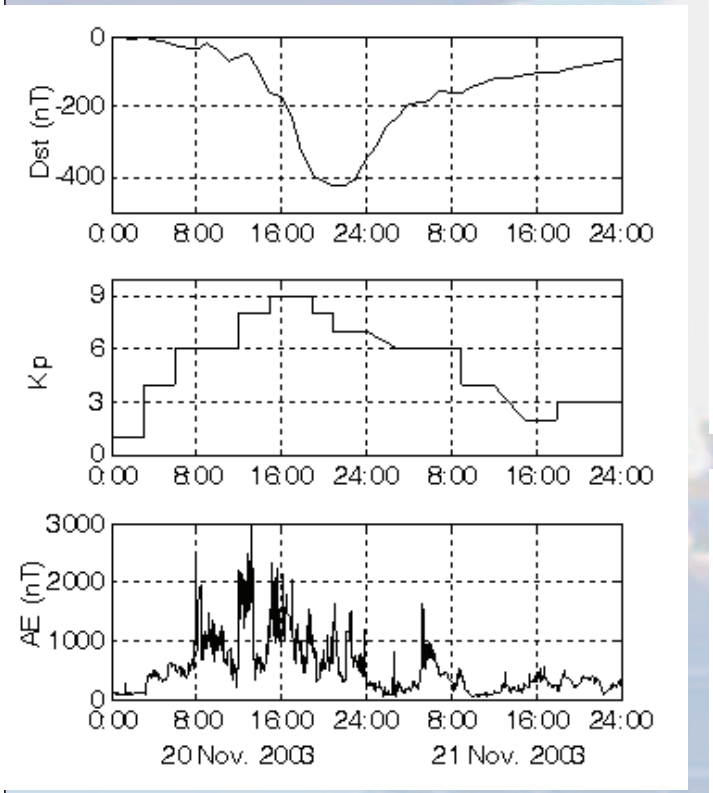

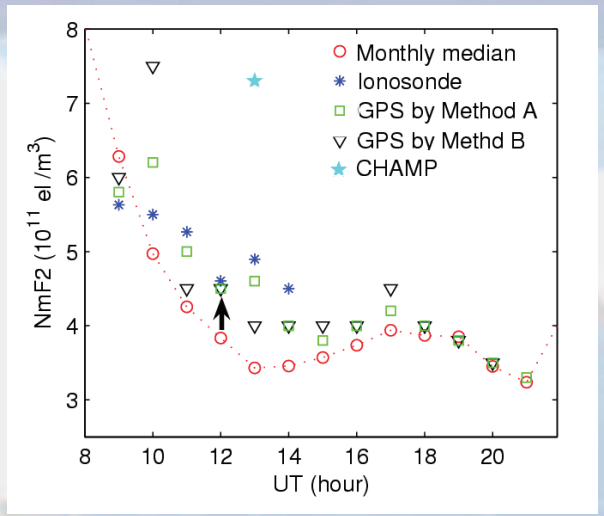

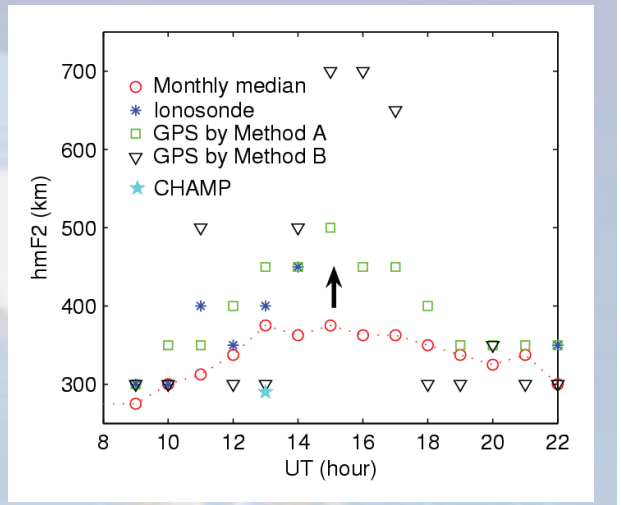

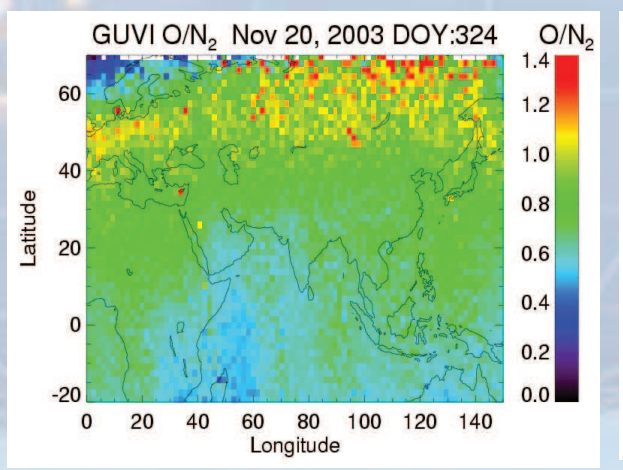

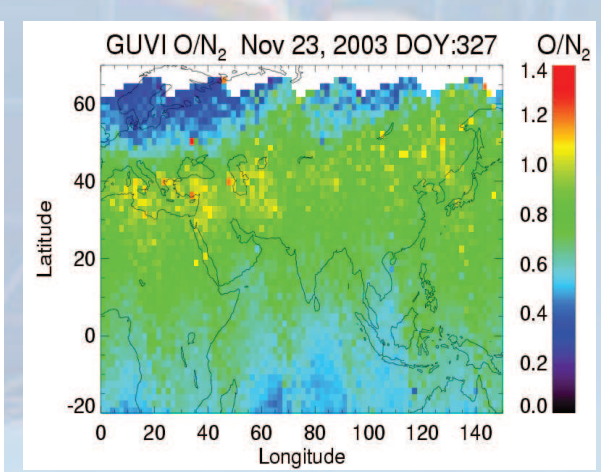

Jin et al., J. Geodesy, 2008.

2.2 Ocean Remote Sensing

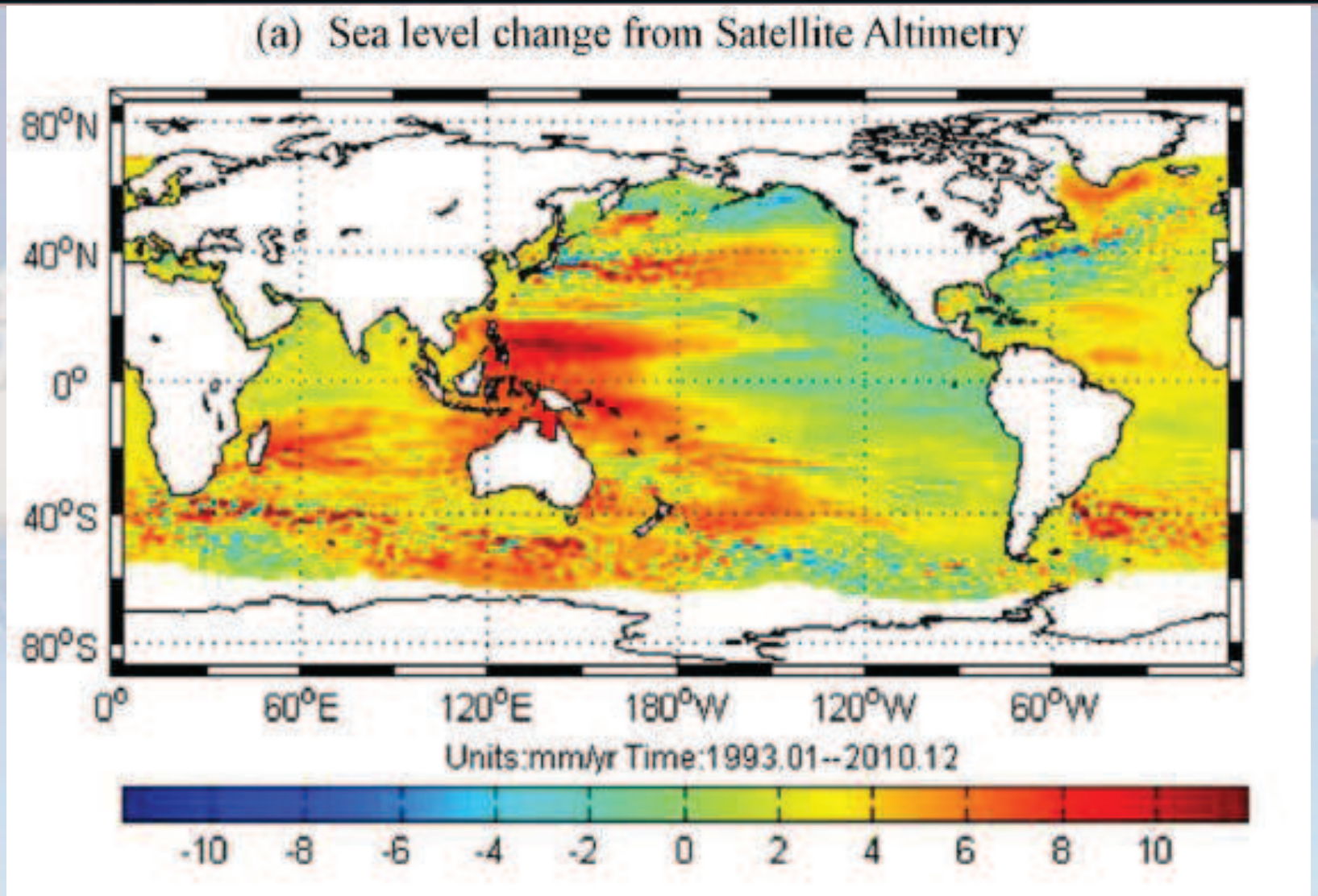

2.3 Hydrological Remote Sensing

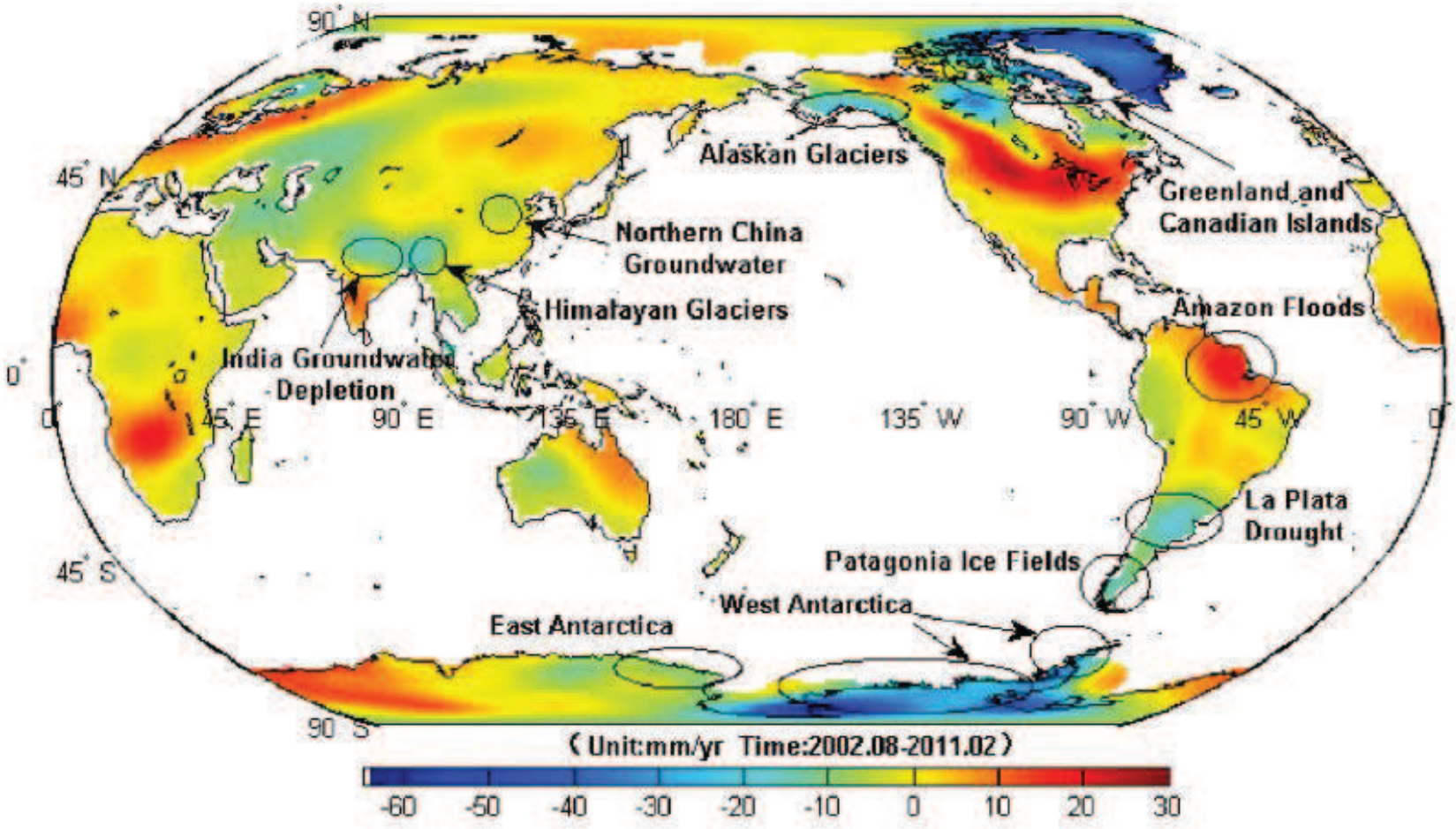

Fig. 6. The trend of terrestrial water storage from GRACE (2002–2011).

Jin et al., J. Geodyn., 2013

2.4 Earthquake/Crustal deformation by GPS/InSAR

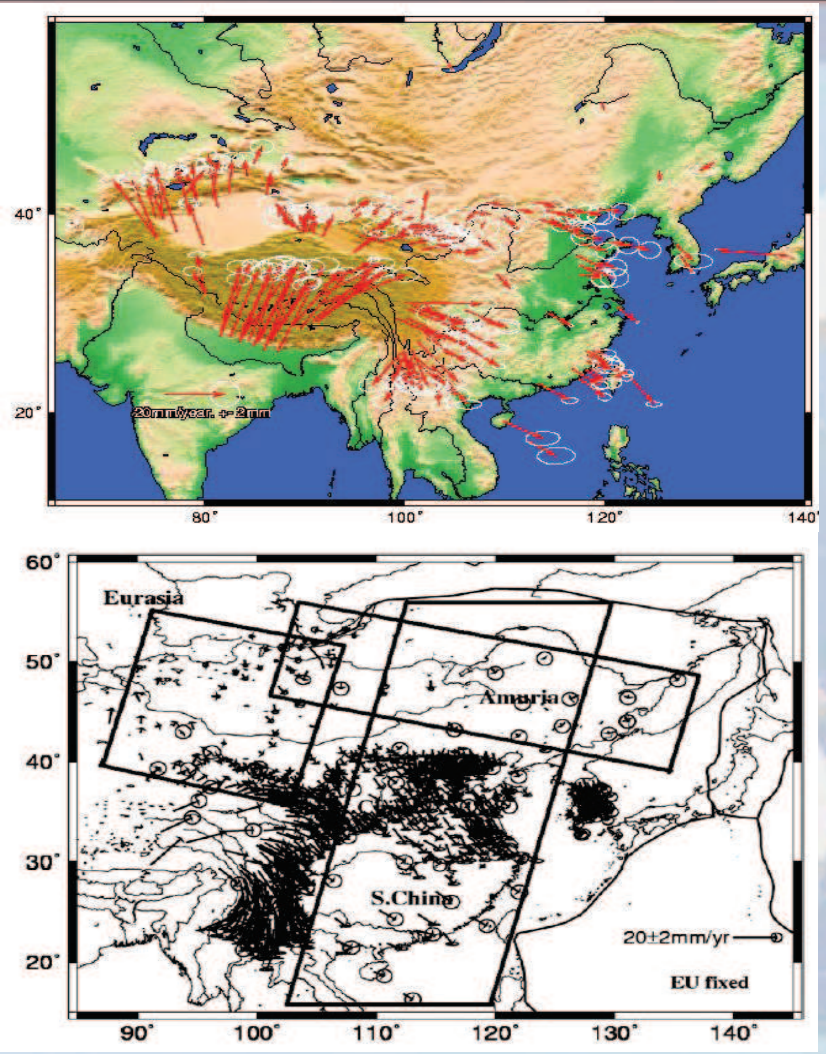

Jin et al. EPSL, 2007

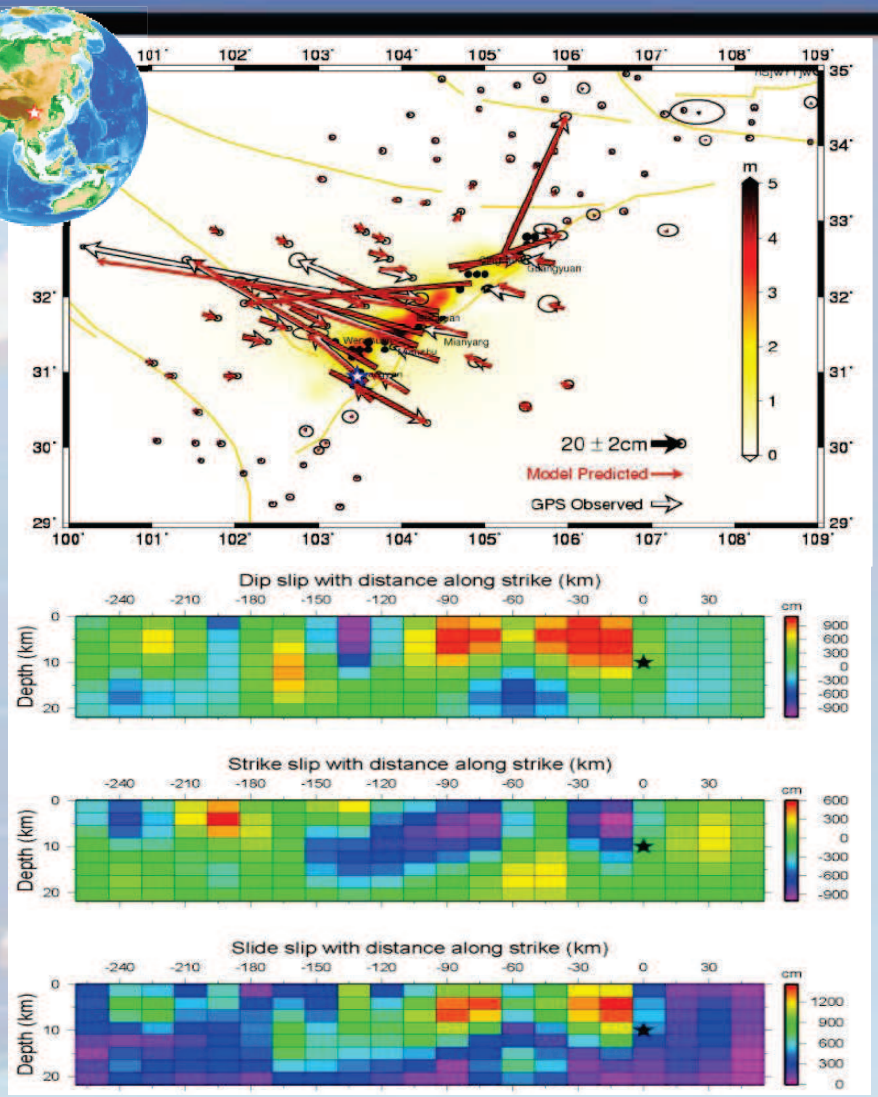

Jin et al., Int. J. Remote Sens. 2010

Co-seismic Ionospheric Disturbance (2008 China Mw=8.0 Earthquake)

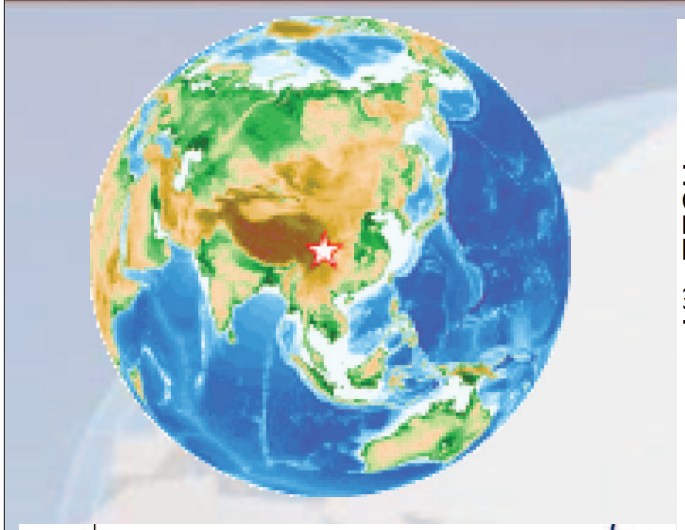

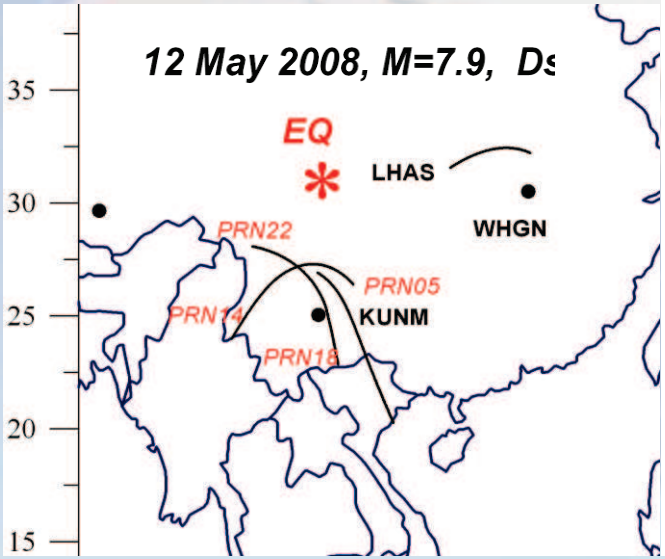

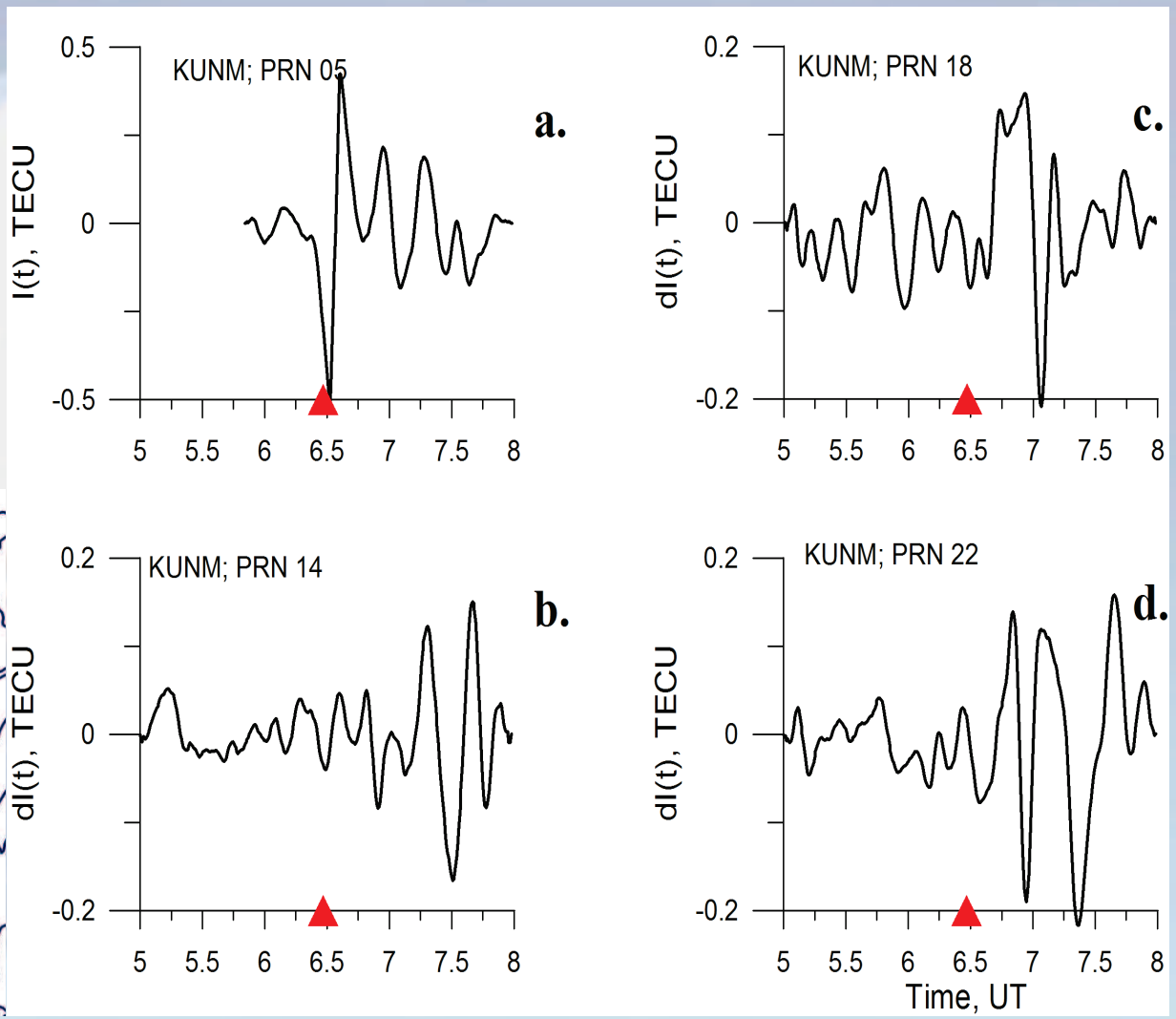

Jin et al., Int. J. Remote Sens., 2010

3. Problems and challenges

- GPS Height precision (e.g. stochastic modeling?)
- GPS ionospheric tomography due to lack of vertical information constraints, requiring more signals, e.g. Galileo, Compass…
- GPS Ionospheric TEC: Coupling with solid-earth activities (e.g. Earthquake)
- Any precursors prior to Earthquakes by Space Geodesy? ….

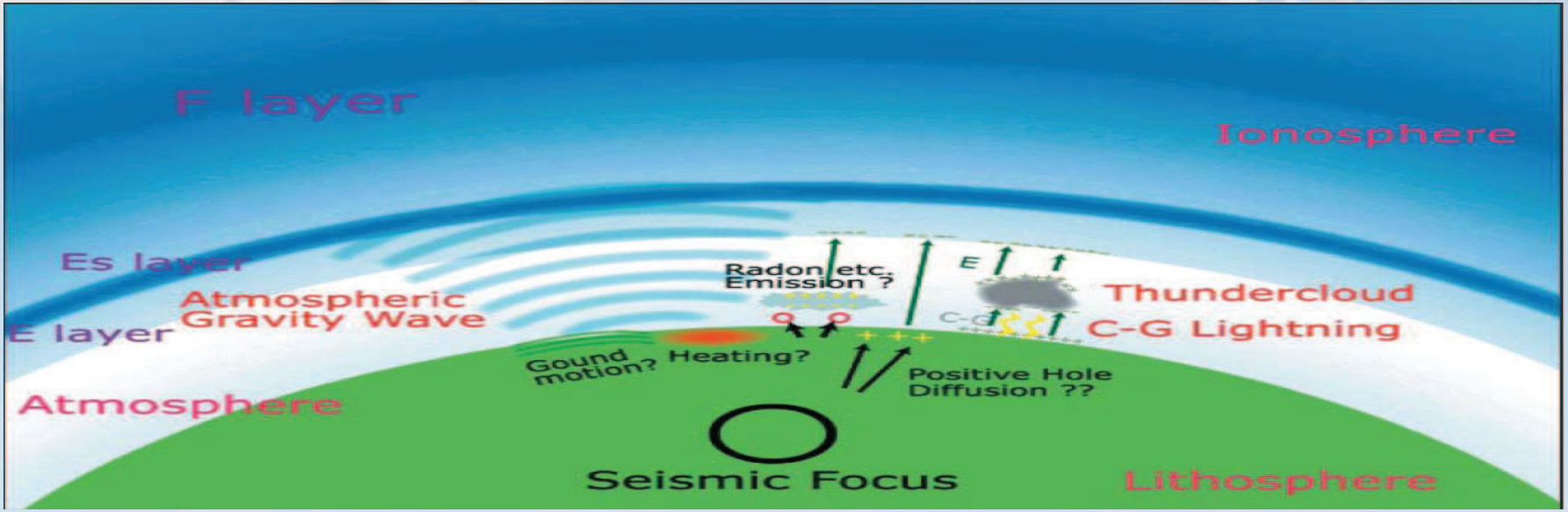

Precursory transient slip during the 2001 Mw = 8.4 Peru earthquake sequences from continuous GPS

- 2-hour GPS position series show that precursory deformation begins 18 hours prior to the July 7 Mw = 7.6 aftershock, especially in North component. This pre-seismic deformation may be caused by slow faulting prior to the Mw = 7.6 aftershock.

Melbourne et al., GRL, 2002

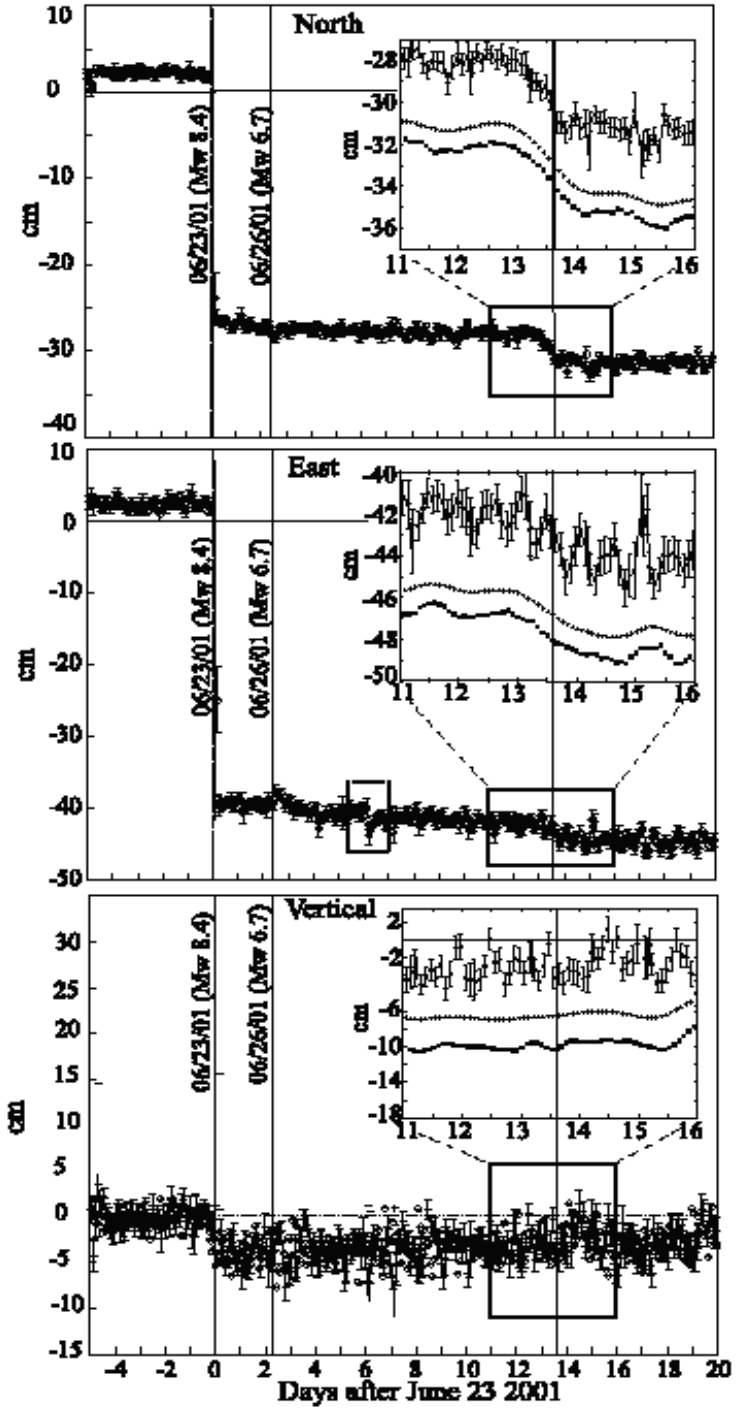

Can GPS detect tectonic activities?
--A case of GPS detection in New Madrid Seismic Zone

- In the winter of 1811−1812, near the town of New Madrid in US, three earthquakes within three months shook the entire eastern half of the country and liquefied the ground over distances far greater than any historic earthquake in North America. Geological evidence demonstrates that liquefaction generated by the New Madrid earthquakes, has occurred at least three and possibly four times in the past 2,000 years, consistent with recurrence statistics derived from regional seismicity.

- Smalley et al. (Nature 2005) showed direct evidence for rapid strain rates in the area determined from a continuously operated global positioning system (GPS) network. Rates of strain are of the order of 10-7 per year, comparable in magnitude to those across active plate boundaries, and are consistent with known active faults within the region. These results have significant implications for the definition of seismic hazard and for processes that drive intraplate seismicity.
- Smalley Jr R.et al., Space geodetic evidence for rapid strain rates in the New Madrid seismic zone of central USA, *Nature,* 435, 1088-1090, 2005.

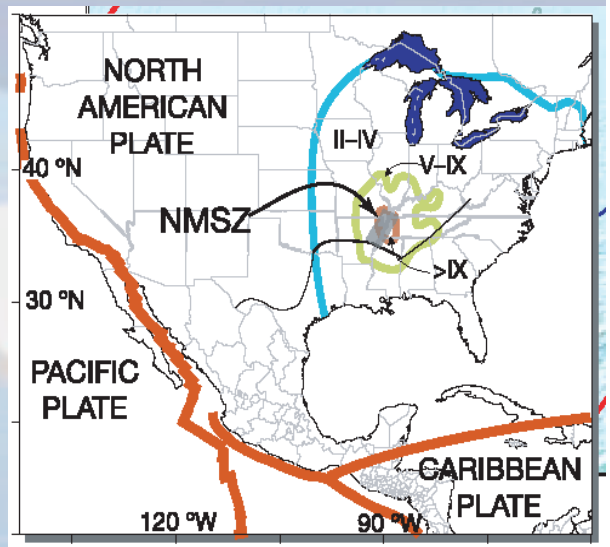

1. Rydelek and Pollitz, GRL, 21, 2302-2306 (1994).
2. Newman et al., Science 284, (1999).
3. Tuttle and Schweig, Geology 23, 361-380 (1995).
4. Kenner and Segall, Science 289 (2000).
5. Nocquet et al., GRL, 32, doi:10.1029/2004GL022174 (2005).
6. Beavan et al., JGR. 107, doi:10.1029/2001JB000282 (2002).

Figure 1 | Velocities and associated uncertainties (95% confidence) at continuous GPS sites in the New Madrid seismic zone. To perform these analyses, two different software packages (GAMIT and GIPSY) were used. Site velocities are within their error ellipses and hence show no statistically significant motion. Filled coloured circles show regional seismicity (United States Geological Survey catalogues; details of site names are listed in Table 1 of ref. 1, except BLMM). The different arrow types represent two independent solutions. Scale bar, 20 km. Inset, time series of daily baseline length estimates between sites RLAP and NWCC after removal of a mean. Error bars on daily estimates, omitted for the sake of clarity, are of the order of 2–3 mm.

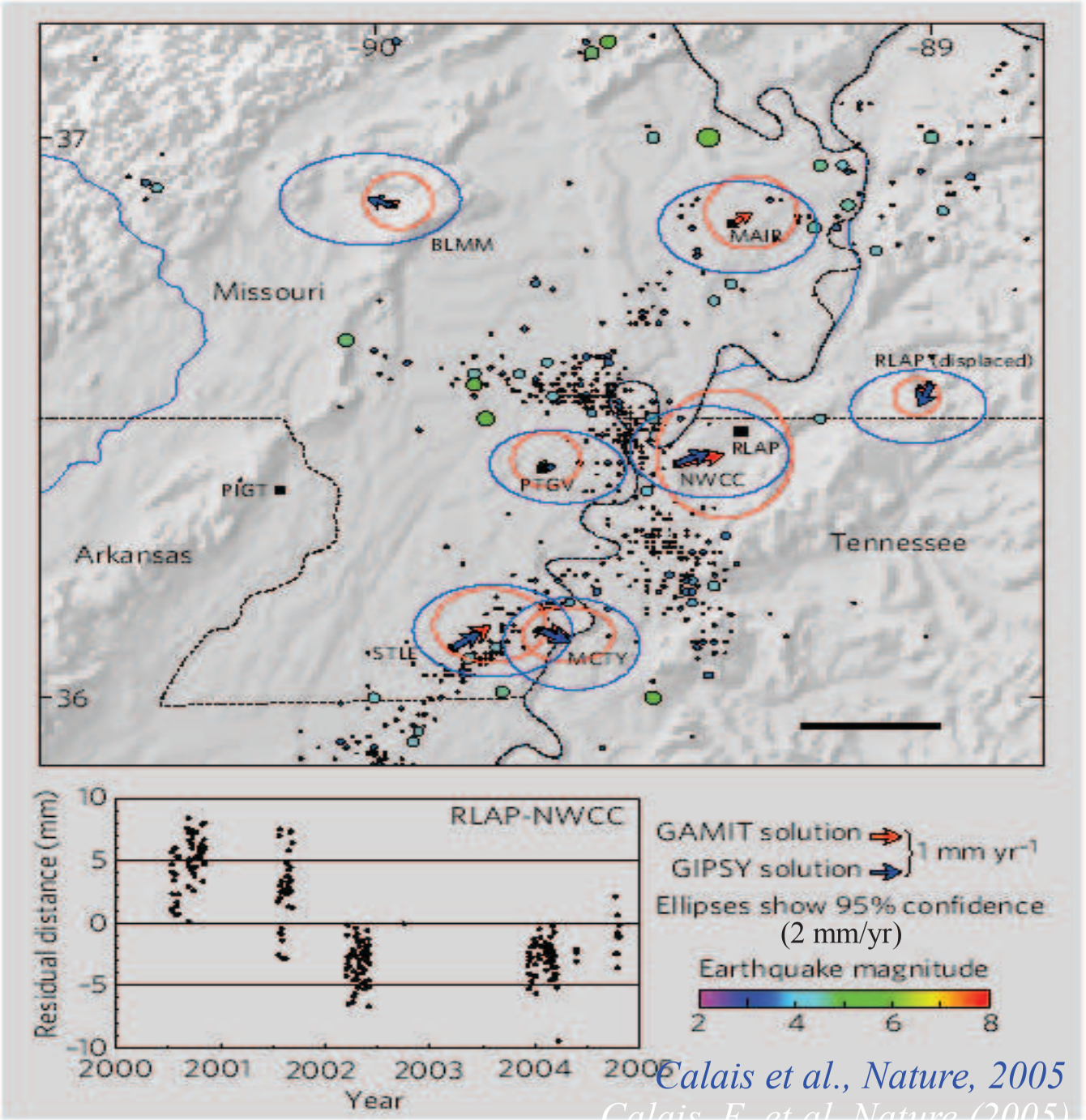

Calais et al., Nature, 2005

Calais, E. et al. Nature (2005)

Thank for your attention!

Prof. Dr. Shuanggen Jin

Email: sgjin@shao.ac.cn
Website: http://www.shao.ac.cn/geodesy